THE JOURNAL OF PHYSICAL CHEMISTRY B LETTERS

2006, *110,* 8921−8923
Published on Web 04/18/2006

Solvent Triggered Change of the Electron Excitation Route of KI in Supercritical NH_3

Germán Sciaini,[†] Ernesto Marceca,[†] and Roberto Fernández-Prini*[,†,‡]

INQUIMAE/DQIAQF, Facultad de Ciencias Exactas y Naturales, Universidad de Buenos Aires, Argentina, and UAQ, Comisión Nacional de Energía Atómica, Argentina

Received: February 21, 2006; In Final Form: March 28, 2006

The UV-spectroscopic behavior of KI contact ion pairs (CIPs) dissolved in supercritical NH_3 was studied combining classical molecular dynamics simulations with electronic structure calculations, and the results show that an abrupt change of the photoexcitation route of KI CIPs occurs at very low solvent densities. Few NH_3 solvating molecules are required to hamper the well-known photoinduced intramolecular electron (e^-) transfer observed in isolated ion pairs of alkali metal halides in the vapor drawing the e^- to solvent cavities leading to a charge-transfer-to-solvent process.

Charge transfer processes are very common, being found in many fields of science that cover condensed-matter physics, chemistry, and biology.[1] Charge transfer processes are generally involved in more complex photoinduced reactions; for this reason, the study of the charge transfer taking place in simple model systems[2] constitutes an important tool for understanding this type of reactions. Although the internal charge transfer which occurs when alkali metal halides are photoexcited in the vapor phase has been extensively analyzed,[3,4] there are only a few spectroscopic studies of contact ion pairs (CIPs) in ammonia and water clusters[5] and, moreover, there is no information available about this process in bulk polar solvents. On the other hand, charge-transfer-to-solvent (CTTS) processes due to the electron photoexcitation of dissolved iodides in bulk polar solvents have been investigated since the 1970s,[6,7] and more recently in clusters.[8] However, although the CTTS process is well established when the iodide is not forming an ion pair, there is no information about the counterion's effect upon the electronic photoexcitation process when the dissolved ions are forming CIPs.

Our previous work on UV-spectroscopic properties of CIPs[9,10] dissolved in supercritical ammonia[11] prompted us to do classical molecular dynamics (MD) simulations combined with electronic structure calculations for a potassium iodide CIP dissolved in bulk NH_3 under supercritical conditions (at a temperature of 420 K and different solvent densities).

Constant-*NVT* molecular dynamics runs with periodic boundary conditions were carried out for one K^+ and one I^- in 215 NH_3 at different solvent densities using the AMBER 8 package.[12] For the NH_3 molecules, the rigid model proposed by Impey and Klein[13] was used. More details about the classical pair potential parameters for K^+-NH_3, I^--NH_3, and K^+-I^- have been given in our previous work.[10] The evolution of the simulated system was followed for 200 ps after 50 ps of equilibration using a time step of 0.4 fs, and 100 randomly selected snapshots of KI CIPs for each solvent density were used to calculate its electronic structure.

The ab initio electronic structure calculations were done for each snapshot using the Gaussian 98 package[14] and then averaged in order to obtain the mean value of some electronic properties for the CIP ground and excited states. Calculations were carried out using single reference methods based on the Hartree−Fock approximation and Möller−Plesset second-order perturbation theory (MP2), and the results were compared with those from configuration interaction single excitation (CIS). We decided to follow the approach proposed by Bradforth and Jungwirth[7] who approximated the singlet excited state for the lowest triplet. This strategy could be used due to the weak association between the excited electron and the nuclear core of iodine, making the energy and electron distribution of the lowest triplet state quite similar to that for the singlet excited state (the energy difference was ∼0.3 eV at all fluid densities, a value which agrees with the observation of Bradforth and Jungwirth).

For the iodine atom, we have employed the LANL2DZ effective core potential with diffuse basis functions. These basis functions for the eight valence electrons of iodide have been augmented by a very diffuse s set with eight exponents forming a geometric series with a factor of 2 and a lowest exponent of 1.406×10^{-3} plus a p set with an exponent of 0.500 and six exponents forming a geometric series with a factor of 2 and a lowest exponent of 4.688×10^{-4} plus a d basis with an exponent of 0.100. The inclusion of the very diffuse basis set was crucial in order to reproduce the iodide electron binding energy, 3.01 eV at the MP2 level versus 3.06 eV from experiment.[15] Moreover, with the quantum representation of iodide employed in the present work and using HF, MP2, and CIS methods, we were able to reproduce exactly the results for the electronic structure calculations of $I^-(H_2O)_2$ and $I^-(H_2O)_6$ clusters obtained by Bradforth and Jungwirth[7] using a different pseudopotential and basis set for I^- .

The potassium atom and the atoms of the solvent molecules, whenever they were considered as quantum molecules, were represented with the corresponding 6-31++G* basis set. We

* Corresponding author. E-mail: rfprini@cnea.gov.ar.
[†] Universidad de Buenos Aires.
[‡] UAQ.

10.1021/jp061110g CCC: $33.50

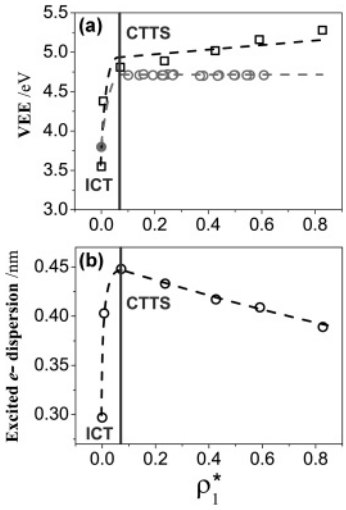

Figure 1. (a) Vertical excitation energy (VEE) against ρ^*_1: open circles, experimental;[10] solid circle, from ref 3; squares, calculated values. (b) Calculated excited electron dispersion. The dashed curves are indicative of the general trends. The vertical solid line at $\rho^*_1 = 0.07$ indicates where the change in the excitation route occurs. ICT denotes internal charge transfer.

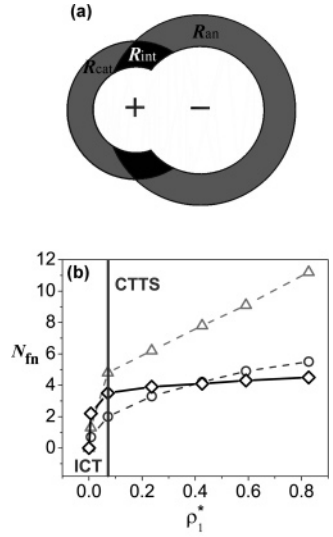

Figure 2. (a) Scheme of the first solvation shell of the CIP; the three regions described in the text are shown. (b) N_{fn} in each region; circles represent the N_{fn} values in R_{cat}, diamonds represent those in R_{int}, and triangles represent those in R_{an}.

obtained for the ionization potential of potassium atom 4.12 eV using MP2; this is in reasonable agreement with the experimental value 4.34 eV.[16]

The use of point-charge solvent molecules has proved successful for describing CTTS transitions of iodide in bulk water.[7] To validate this assumption for our system, we have compared the electronic structure calculation results obtained using a quantum representation for the NH_3 molecules in the first solvation shell with those obtained using the point-charge distribution proposed by Impey and Klein[13] for those molecules. The typical differences in the vertical excitation and electron radial extent (vide infra) were found to be ~0.2 eV and ~0.03 nm, respectively, being much smaller than the usual dispersion of these quantities due to solvent configuration fluctuations (~0.5 eV and ~0.05 nm). Therefore, we decided to describe all solvent molecules as a point-charge distribution which was found to be sufficient to reproduce the electronic properties of our system with good precision and in a reasonable CPU time. Further details about the validation procedure will be given in a forthcoming article.

Our results reveal that the photoinduced electron transfer mechanism switches sharply at very low NH_3 density. The well-known photoinduced internal charge transfer taking place in alkali metal halide ion pairs in vacuum is rapidly replaced by a CTTS-like process in the presence of a few NH_3 solvating molecules. For KI in vacuo, the excited electron distribution is localized around the K^+ center (internal charge transfer), whereas it shifts toward the iodine atom and has a more extended distribution (CTTS level) as the fluid density increases.

This change in the photoexcitation route is reflected by abrupt changes in many solvent-averaged electronic properties of KI CIPs; two of the most representative ones are depicted in Figure 1 as a function of the reduced NH_3 density (ρ^*_1).[17] The figure shows the ρ^*_1 dependence of the experimental[10] and calculated vertical electronic photoexcitation energy (VEE), panel a, and the excited electron (e^-) dispersion, panel b. The VEE is the energy required to excite the electron in the solvated CIP, and the excited e^- dispersion gives an idea of its instantaneous spatial extent. The excited e^- dispersion was estimated as $\langle\sqrt{\langle r_e^{-2}\rangle - \langle r_e^{-}\rangle^2}\rangle$. The excited electron square radial distribution $\langle r_e^{-2}\rangle$ was taken as the difference between those for the excited state and the core (after electron detachment), that is, in terms of wave functions, $\langle r_e^{-2}\rangle = \langle\Psi_{exc.st.}|r^2|\Psi_{exc.st.}\rangle - \langle\Psi_{core}|r^2|\Psi_{core}\rangle$. The mean excited e^- distance to the center of coordinates $\langle r_e^{-}\rangle$ was calculated using the K^+-e^- mean distance, given by μ/q_{e^-} (where μ is the dipole moment of the CIP excited state and q_{e^-} is the e^- charge). The origin of coordinates was located at the atomic number weighted distance between K and I atoms.

It can be seen that even an incipient solvation produces a strong variation of both properties until ρ^*_1 reaches a value of ~0.07; this value depends to a small extent on the intermolecular potential used for NH_3. The observed behavior is a clear indication that a new electron photoexcitation route has been established around $\rho^*_1 = 0.07$. When $\rho^*_1 > 0.07$, photoexcitation promotes the e^- to solvent cavities in the first solvation shell and, as expected, a further increase of ρ^*_1 reduces the spatial extension of the excited e^- which becomes progressively confined, as indicated by the decrease of its dispersion (see Figure 1b).

The change of the photoexcitation route is a consequence of solvation; hence, to analyze this phenomenon, it is convenient to divide the first solvation shell of the CIP in different regions. Figure 2 shows the different solute−solvent interaction regions around the CIP, panel a, and the number of first-neighbor NH_3 molecules (N_{fn}) in each region,[18] panel b. R_{int} represents the region where the first solvation shells of the two ions intersect each other, and R_{cat} and R_{an} are the cation-side and anion-side solvation regions, respectively.

The solvent molecules in R_{int} are oriented by the solute's force field so that they interact favorably with both ions, positioning their negative N end toward the K^+ center and its positive H end toward the I^- center. The approximate values for the KI−NH_3 pair interaction energy for each region are −0.7 eV in R_{int}, −0.4 eV in R_{cat}, and −0.1 eV in R_{an}. In R_{cat} and R_{an}, the presence of the counterions reduces the NH_3 ion interaction energy to about half of its value in the absence of the counterion; in particular, the I^-−NH_3 interaction energy in the CIP becomes as small as that found between two ammonia molecules.[19] It should be noted that once the new photoexcitation route is established the behavior of N_{fn} as a function of ρ^*_1 reflects the

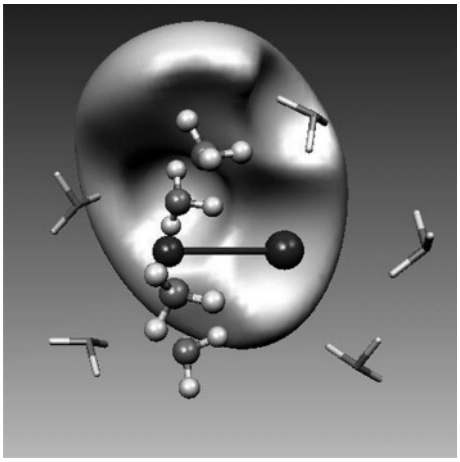

Figure 3. Illustrative picture of the excited e^- in the CIP. The NH_3 molecules located in R_{int} forming the wedged structure are depicted by balls and sticks to distinguish them from the other NH_3 first neighbors (depicted by sticks). K^+ is on the left-hand side and I atom on the right-hand side.

effect of the different $KI-NH_3$ interaction energy magnitudes found for each region. The N_{fn} value in R_{an} increases linearly with ρ^*_1, whereas it tends to a limiting value around 5 or 6 in R_{cat} when ρ^*_1 approaches liquidlike values. The N_{fn} value in R_{int} rapidly ($\rho^*_1 \sim 0.07$) reaches a constant value corresponding to four NH_3 molecules wedged in a girdle structure around the CIP internuclear axis, as shown in Figure 3, where the shape and localization of the e^- in the solvated CIP excited state are illustrated for a representative MD snapshot at $\rho^*_1 = 0.07$.

The reason for the observed solvent density independence of the VEE when $\rho_1^* > 0.07$ (see Figure 1a) can be understood on the basis of the scheme shown in Figure 2a. The solvent molecules located in R_{cat} stabilize both the ground state and vertical electronic excited state to a similar extent because these molecules interact mostly with a K^+-like center. Moreover, the NH_3 molecules in R_{an} have a negligible effect due to the cation's proximity in the CIP, as shown also by the almost constant value of ~7.5 eV obtained for the ionization potential of the CIP as a function of ρ_1^*. These arguments also explain the near independence of the VEE with size reported for small $NaI(NH_3)_n$ and $NaI(H_2O)_n$ clusters.[5]

In summary, the formation of a doubly anchored solvating wedge consisting of four NH_3 molecules surrounding the CIP's internuclear axis appears fundamental to change the photoexcitation route from an internal charge transfer to a CTTS directing the excited e^- to solvent cavities. The cation's presence has an important influence on the solvent structure, and the solvated CIP electronic excited state differs from that found in vacuum; cation−solvent stabilization cannot be ignored when describing the photoexcitation process. The very low ρ_1^* value at which the change of route occurs is a salient feature of ionic solvation also affecting other properties, for example, the change of the solute's chemical potential with ρ_1^*.[9] Thus, for ionic systems in polar solvents, including water, where solute−solvent interactions are strong, the behavior at very low fluid density is very important to connect the properties in the solutions with those of the solute vapor ($\rho^*_1 \rightarrow 0$).

Acknowledgment. We thank Professor D. Estrin (UBA, Argentina) for helpful comments about ab initio calculations. We are grateful for partial economic support given by ANPCyT (PICT 6818) and UBACyT (X-218/330). E.M. and R.F.-P. are members of the Carrera del Investigador (CONICET, Argentina), and G.S. thanks CONICET (Argentina) for a doctoral fellowship.

References and Notes

(1) (a) Fox, M. A. *Chem. Rev.* **1992**, *92*, 365. (b) Davidson, V. L. *Biochemistry* **2002**, *41*, 14634.

(2) Martini, I. B.; Barthel, E. R.; Schwartz, B. J. *Science* **2001**, *293*, 462.

(3) Davidovits, P.; Brodhead, D. C. *J. Chem. Phys.* **1967**, *46*, 2968.

(4) (a) Berry, R. S. In *Alkali Halide Vapors*; Davitovits, P., McFadden, D. L., Eds.; Academic: New York, 1979; see also references therein for earlier work. (b) Foth, H. J.; Polanyi, J. C.; Telle, H. H. *J. Phys. Chem.* **1982**, *86*, 5027. (c) Rose, T. S.; Rosker, M. J.; Zewail, A. H. *J. Chem. Phys.* **1989**, *91*, 7415.

(5) (a) Grégoire, G.; Mons, M.; Dimicoli, I.; Dedonder-Lardeux, C.; Jouvet, C.; Martrenchard, S.; Solgadi, D. *J. Chem. Phys.* **1999**, *110*, 1521. (b) Grégoire, G.; Mons, M.; Dimicoli, I.; Dedonder-Lardeux, C.; Jouvet, C.; Martrenchard, S.; Solgadi, D. *J. Chem. Phys.* **2000**, *112*, 8794. (c) Dedonder-Lardeux, C.; Grégoire, G.; Jouvet, C.; Martrenchard, S.; Solgadi, D. *Chem. Rev.* **2000**, *100*, 4023.

(6) (a) Blandamer, M. J.; Fox, M. F. *Chem. Rev.* **1970**, *70*, 59. (b) Sheu, W. S.; Rossky, P. J. *Chem. Phys. Lett.* **1993**, *213*, 233. (c) Staib, A.; Borgis, D. *J. Chem. Phys.* **1996**, *104*, 9027. (d) Sheu, W. S.; Rossky, P. J. *J. Phys. Chem.* **1996**, *100*, 1295.

(7) Bradforth, S. E.; Jungwirth, P. *J. Phys. Chem. A* **2002**, *106*, 1286.

(8) (a) Serxner, D.; Dessent, C. E.; Johnson, M. A. *J. Chem. Phys.* **1996**, *105*, 7231. (b) Greenblatt, B. J.; Zanni, M. T.; Neumark, D. M. *Discuss. Faraday Soc.* **1997**, *108*, 101. (c) Lehr, L.; Zanni, M. T.; Frischkorn, C.; Weinkauf, R.; Neumark, D. M. *Science* **1999**, *284*, 635. (d) Elola, M. D.; Laria, D. *J. Chem. Phys.* **2002**, *117*, 2238.

(9) Sciaini, G.; Marceca, E.; Fernández-Prini, R. *J. Supercrit. Fluids* **2005**, *35*, 106.

(10) Sciaini, G.; Marceca, E.; Fernández-Prini, R. *J. Phys. Chem. B* **2005**, *109*, 18949.

(11) The critical parameters for NH_3 are the following: critical pressure, 11.333 MPa; critical temperature, 405.4 K; critical density, 13.218 mol·dm^{-3}.[9] The UV-spectroscopic experiments were carried out using a high pressure cell. The temperature was fixed at 420 K with a PID electrical control system, and a manual pump with pressure transducers was used in order to obtain the desired density. The KI concentrations were around 10^{-5} mol·dm^{-3}; for more details, see ref 10.

(12) Case, D. A.; Darden, T. A.; Cheatham, T. E., III; Simmerling, C. L.; Wang, J.; Duke, R. E.; Luo, R.; Merz, K. M.; Wang, B.; Pearlman, D. A.; Crowley, M.; Brozell, S.; Tsui, V.; Gohlke, H.; Mongan, J.; Hornak, V.; Cui, G.; Beroza, P.; Schafmeister, C.; Caldwell, J. W.; Ross, W. S.; Kollman, P. A. *AMBER 8*; University of California: San Francisco, CA, 2004.

(13) Impey, W.; Klein, M. L. *Chem. Phys. Lett.* **1984**, *104*, 579.

(14) Frisch, M. J.; Trucks, G. W.; Schlegel, H. B.; Scuseria, G. E.; Robb, M. A.; Cheeseman, J. R.; Zakrzewski, V. G.; Montgomery, J. A., Jr.; Stratmann, R. E.; Burant, J. C.; Dapprich, S.; Millam, J. M.; Daniels, A. D.; Kudin, K. N.; Strain, M. C.; Farkas, O.; Tomasi, J.; Barone, V.; Cossi, M.; Cammi, R.; Mennucci, B.; Pomelli, C.; Adamo, C.; Clifford, S.; Ochterski, J.; Petersson, G. A.; Ayala, P. Y.; Cui, Q.; Morokuma, K.; Malick, D. K.; Rabuck, A. D.; Raghavachari, K.; Foresman, J. B.; Cioslowski, J.; Ortiz, J. V.; Stefanov, B. B.; Liu, G.; Liashenko, A.; Piskorz, P.; Komaromi, I.; Gomperts, R.; Martin, R. L.; Fox, D. J.; Keith, T.; Al-Laham, M. A.; Peng, C. Y.; Nanayakkara, A.; Gonzalez, C.; Challacombe, M.; Gill, P. M. W.; Johnson, B. G.; Chen, W.; Wong, M. W.; Andres, J. L.; Head-Gordon, M.; Replogle, E. S.; Pople, J. A. *Gaussian 98*; Gaussian, Inc.: Pittsburgh, PA, 1998.

(15) Hotop, H.; Lineberger, W. C. *J. Phys. Chem. Ref. Data* **1985**, *14*, 731.

(16) Lias, S. G.; Bartmess, J. E.; Liebman, J. F.; Holmes, J. L.; Levin, R. D.; Mallard, W. G. *J. Phys. Chem. Ref. Data* **1988**, *17* (Suppl. 1).

(17) We have chosen the triple point liquid density of NH_3 ($\rho_{1T} = 42.3$ mol·dm^{-3}) to reduce the solvent density values in order to give the idea of the proximity to the liquid phase; thus, $\rho_1^* = \rho_1/\rho_{1T}$.

(18) Values for N_{fn} were obtained by averaging more than 1500 MD snapshots. N_{fn} in R_{int} was obtained by averaging the number of NH_3 molecules having the N center at distances smaller than 0.40 nm from the K^+ center and at the same time distances smaller than 0.55 nm from the I^- center. The N_{fn} values in R_{cat} and in R_{an} correspond to all first-neighbor NH_3 molecules not belonging to R_{int}. The distances used for defining the regions correspond to the first minima of the radial distribution functions of the nitrogen atom in ammonia for each of the ions.

(19) Hinchliffe, A.; Bounds, D. G.; Klein, M. L.; McDonald, I. R.; Righini, R. *J. Chem. Phys.* **1981**, *74*, 1211.